Origin and Nonuniversality of the Earthquake Interevent Time Distribution

Sarah Touati,* Mark Naylor, and Ian G. Main

School of GeoSciences, University of Edinburgh, Grant Institute, The King's Buildings, West Mains Road, Edinburgh EH9 3JW, United Kingdom

(Received 9 January 2009; published 24 April 2009)

Many authors have modeled regional earthquake interevent times using a gamma distribution, whereby data collapse occurs under a simple rescaling of the data from different regions or time periods. We show, using earthquake data and simulations, that the distribution is fundamentally a bimodal mixture distribution dominated by correlated aftershocks at short waiting times and independent events at longer times. The much-discussed power-law segment often arises as a crossover between these two. We explain the variation of the distribution with region size and show that it is not universal.

DOI: 10.1103/PhysRevLett.102.168501 PACS numbers: 91.30.Px, 02.50.Ey, 89.75.Da, 91.30.Dk

Over the past decade, much scientific attention has been focused on the distribution of waiting times between earthquake events within a region or catalog [1–6], whose form and origin have great importance for the development of physical or statistical models of earthquake dynamics. Most authors have explored these interevent times by fitting the empirical histograms to a gamma distribution, which has led to the suggestion of universality [1–3,7,8], even down to the scale of laboratory rock fracture experiments [9]. The idea that has enthusiastically been pursued is that a rescaling involving region size and magnitude cutoff [1], or simply the mean event rate [2], produces data collapse onto a universal gamma distribution. Much of this analysis, however, has been restricted to the use of data with an apparently stationary event rate (e.g., [2,8]) since mean event rates are otherwise poorly constrained; there is some evidence that nonstationary data analyzed in the method of Bak *et al.* do not collapse [10]. Further, it is common also to omit the shortest interevent times from the analysis [1,2]; if these interevent times are included, the approximate data collapse is broken [4]. These common restrictions tend to filter out high rates of aftershocks and thereby introduce a strong selection bias in the data, leading us to question the proposed universality. Recent analytic studies on the Epidemic-Type Aftershock Sequences (ETAS) model, a process-based stochastic earthquake occurrence model [11], have indicated that the interevent time distribution is not universal, but may be approximately universal under some circumstances [12,13].

We first explore afresh the structure of global and regional earthquake interevent time series, then demonstrate how the observed range of interevent time distributions arise from well-known empirical laws of seismicity by presenting comparative results from simulations of the ETAS model. We show that the form of the interevent time distribution in both earthquake catalogs and simulations is generally bimodal, and is best described as a mixture distribution, formed by the different patterns associated with correlated and uncorrelated event pairs. The frequently cited power-law segment in the distribution [1,2,4] arises as a crossover between the two peaks of these distributions. Support for bimodality in the distribution can also be found in published literature involving real data [4,14], simulations [15], and analytic studies on the ETAS model [16], although no comment has, up to now, been made on the bimodal shape. We draw attention to it and present a physically-motivated, intuitive explanation for its origin.

Simulations also provide a way around the stationarity problem and allow us definitively to reject the hypothesis of universality. While on short time scales the earthquake rate is inherently nonstationary, earthquakes in the long term are a stationary, albeit nonlinear process; their event rate converges slowly but definitely onto a well-defined value [17]. Using lengthy ETAS simulations, we are able to include strong aftershock activity in our interevent time sequence and still confidently define a mean event rate. This is akin to using a small region (such as Southern California) but recording data for a very long time. As expected from the bimodality, the distributions only approximately rescale with the mean event rate when including a wider range of realistic seismic patterns in the analysis than is available currently in real catalogs [17,18].

Interevent time histograms for a global and a regional (Southern California) catalog are shown in Fig. 1. Our preferred way for plotting the data is shown in the left hand figures in which a clear distinction can be seen between the global data, which forms a single-peaked distribution, and the regional distribution, which appears more bimodal. More commonly, interevent time distributions are plotted in the form of the right hand figures where each frequency has been normalized by the bin width, which tends to smooth out the two bumps so they cannot readily be distinguished as such [Fig. 1(b) and 1(d)]. They can however be seen in some rescaled plots in the literature (e.g., [4]). It is important to highlight the evidence that these are real features and that the much-discussed gamma distribution is in fact only an approximate description of the interevent time histogram.

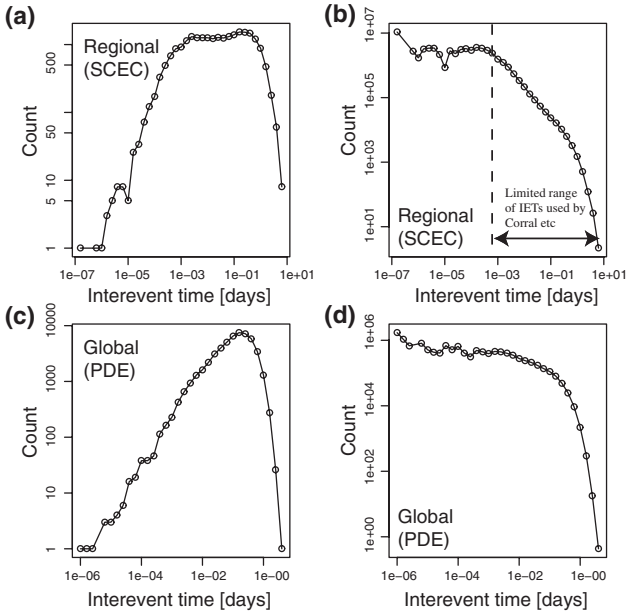

FIG. 1. Interevent time histogram for the Southern California Earthquake Center (SCEC) catalog, plotted (a) without and (b) with normalization by the bin widths. Events larger than magnitude 2.4 between 1984 and 2000 were used. Interevent time histogram for the worldwide Preliminary Determination of Epicenters (PDE) catalog, plotted (c) without and (d) with normalization by the bin widths. Events larger than magnitude 5.0 between 1970 and 2006 were used.

We will now explain these observations using synthetic catalogs generated by the ETAS model. This is a stochastic point-process model in which independent seeding events (sometimes described as background events) occur as a Poisson process in time with constant rate μ, and all past events above a threshold magnitude M_0 may produce aftershocks. The magnitudes of all events are picked independently from the power-law Gutenberg-Richter distribution,

$$\log N = a - bm, \tag{1}$$

where N is the number of events in a given time period with magnitude $\geq m$, and a and b are constants. The model incorporates the empirical observation that events tend to cluster in time due to the time-dependent relaxation of the crust by the release of triggered aftershocks, whose rate $n(t)$ decays as a power law in time after a sizeable event according to the Omori law,

$$n(t) = \frac{K}{(c+t)^p}, \tag{2}$$

where K, c, and p are constants and t refers to time. Aftershock productivity depends exponentially on the magnitude of the parent event so that larger events trigger a greater number of aftershocks. Combining these relations defines the conditional intensity function λ for the ETAS model,

$$\lambda(t|H_t) = \mu + A \sum_{i\, t<t_i} \exp[\alpha(m_i - M_0)]\left(1 + \frac{t-t_i}{c}\right)^{-p}, \tag{3}$$

where t_i are the times of the past events and m_i are their magnitudes. Thus, the five ETAS parameters are μ, the independent event rate, c, p, and $A = K/c^p$, the Omori parameters, and α, the productivity parameter. The model does not make an arbitrary distinction between foreshocks, mainshocks, and aftershocks, but rather regards all events as capable of triggering further events according to these simple rules. Thus, each independent event may result in a cascade of nested aftershock sequences. We refer to such a cascade as a global aftershock sequence, following previous authors [19].

In order to make comparisons with global and regional earthquake data, we concentrate on the rate of independent events, μ, which is effectively the average frequency for which global aftershock sequences are initiated. This parameter can be considered as a proxy for region size; increasing μ increases the extent to which global aftershock sequences overlap in time (Fig. 2), with the effect that a smaller proportion of the events that follow a given event within a certain time period are correlated with it, as is known to be the case for larger regions [20]. Because of the spatial heterogeneity of earthquake occurrence, the

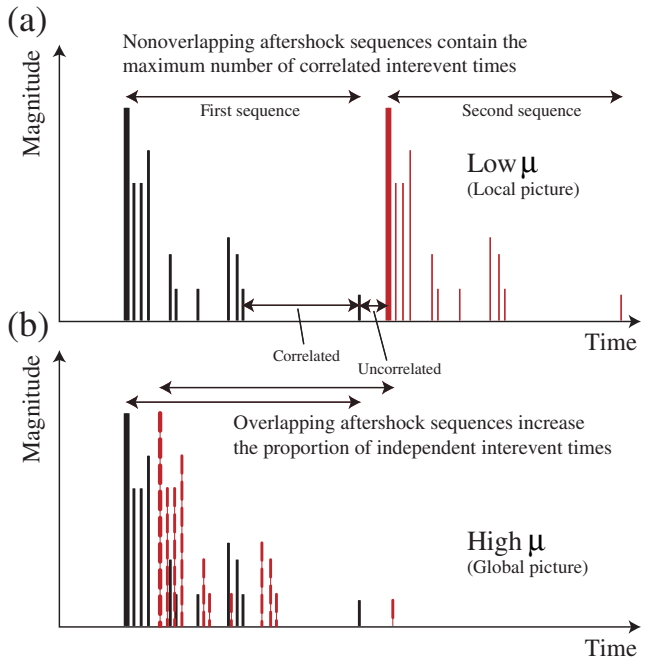

FIG. 2 (color online). Cartoon illustrating how varying the independent event rate changes the proportion of correlated to independent interevent times as a consequence of the degree of overlap of triggered aftershock sequences. (a) Regional catalogs tend to resolve aftershock sequences; (b) Because of the increased independent event rate, global catalogs tend to contain more temporal overlapping and thus more independent interevent times.

actual relation between region size and effective μ will be nonlinear, but this is beyond the scope of this Letter.

The effect of μ on the synthetic ETAS interevent time distribution is shown in Fig. 3. For large μ, the shape of the distribution is similar to that of a Poisson process. For intermediate values of μ, the peak of the distribution flattens out, and we see the familiar gamma distribution. When μ is made very small, however, the straight segment becomes peaked in two places [Fig. 3(a)]. Thus, as we decrease μ, we progress from a unimodal to a bimodal distribution, comparable to the progression from global to regional scale in real data [compare Fig. 3(a) with Figs. 1(a) and 1(c)].

The ETAS model allows us to perform further analysis since we have knowledge of whether each event is independent or triggered. We may therefore categorize each interevent time as either correlated, defined as occurring between two events belonging to the same global aftershock sequence, or uncorrelated, occurring between events of different aftershock sequences (see Fig. 2). Figure 4 shows these correlated and uncorrelated subsets superimposed onto the histograms, for various different values of μ. It is clear that the complicated distribution arises as the sum of two physically motivated distributions which have much simpler forms. The uncorrelated waiting times are Poisson distributed, as expected for independent events. The distribution of correlated waiting times, shown most clearly in Fig. 4(d), has three segments: an exponential increase towards a peak at short interevent times (which is omitted from many published distribution plots), a power-law decay segment, and an exponential tailoff at longer times.

The variation of μ produces a variation in (i) the position of the tailoff in the correlated distribution, and (ii) the relative sizes of the two subsets. This effect arises from the interference of temporally overlapping aftershock sequences (Fig. 2). As μ is increased, fewer aftershocks are allowed to occur before each sequence is "interrupted" by the onset of a new global sequence; the sequence of course continues, but its power-law signature in the interevent time series does not. The range of shapes arising from combinations of these two simpler forms means that we are able qualitatively to describe the distribution of earthquake interevent times as a function of a single reduced parameter: the ratio of consecutive independent to dependent events.

The approximate gamma function used to model the overall interevent time distribution is not directly related to the gamma distribution of correlated events; the effective power-law exponent for the former would depend on the relative heights of the two distributions. This exponent is therefore not directly related to the Omori p parameter, but would be expected to change with the other parameters as well in a complicated way.

Since it has become clear that the distribution is not strictly a gamma distribution, the scaling relation proposed by Corral obviously breaks down (Fig. 5). Note that we have only considered variations of the seeding rate μ without changing the branching ratio. Given that the rate of exponential decay at long interevent times is equal to the fraction of independent events in the catalog [21], and that the power-law slope for correlated events depends on the

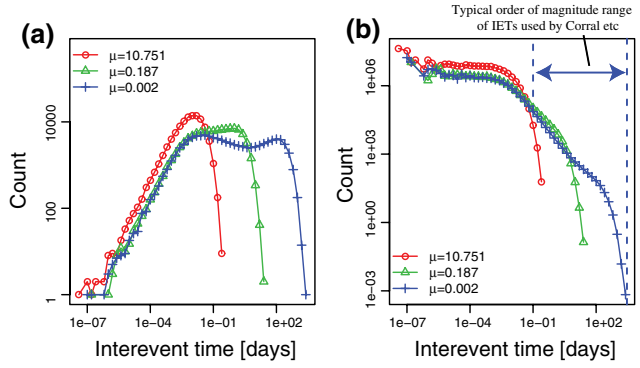

FIG. 3 (color online). Synthetic interevent time histograms for three ETAS simulations with μ values as indicated, plotted (a) without and (b) with normalization by the bin widths. These few examples demonstrate the range of behavior observed in real earthquake interevent time distributions (Fig. 1). The other ETAS parameters used were $A = 10$, $\alpha = 1$, $c = 0.01$, and $p = 1.2$.

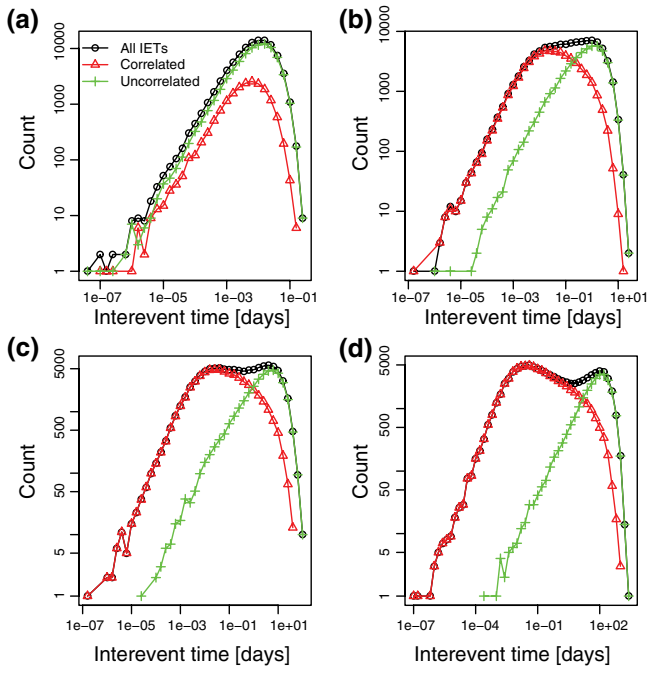

FIG. 4 (color online). Interevent time histograms for four ETAS simulations with μ values (a) 10.751, (b) 0.187, (c) 0.047, and (d) 0.002, plotted without normalization by the bin widths. Correlated (triangle) and uncorrelated (cross) interevent times are shown together with their sum, all interevent times (circle). The other ETAS parameters used were $A = 10$, $\alpha = 1$, $c = 0.01$, and $p = 1.2$.

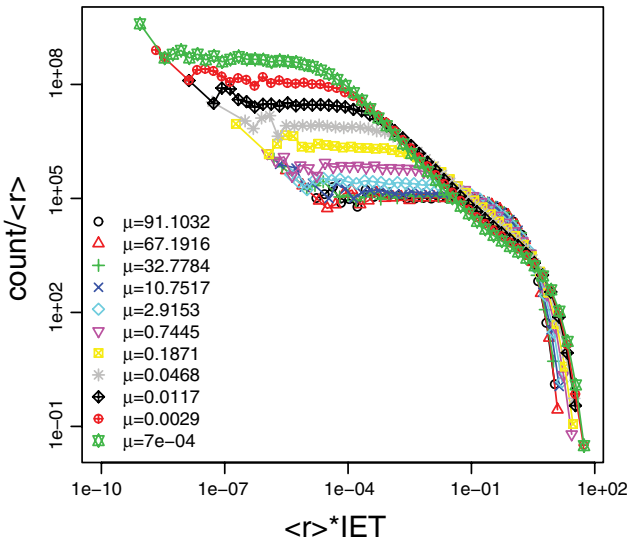

FIG. 5 (color online). Interevent time (IET) histograms for 11 ETAS simulations with μ values as indicated, plotted with normalization by the bin widths, rescaled by the mean event rate r in the manner of Corral. Data collapse is not observed. The other ETAS parameters used were $A = 10$, $\alpha = 1$, $c = 0.01$, and $p = 1.2$.

parameter p [15,21,22], changing the other parameters would be expected to further degrade the data collapse. Raising the lower magnitude cutoff would also alter the shape of the distribution somewhat.

Using the ETAS model and varying the rate of independent events, μ, has allowed us to explore the range of temporal seismicity patterns that result from changing the region size. We have shown that the interevent time distribution is best described as a mixture distribution. It arises as the sum of two contributions: gamma-distributed waiting times between correlated event pairs, those belonging to the same aftershock sequence, at short waiting times; and exponentially distributed times between uncorrelated events at longer times. The larger the region considered, the higher the initiation rate of independent sequences, and so the deeper the interleaving of separate aftershock sequences within the earthquake time series; sequential events are thus more likely to be independent of each other in catalogs from larger regions, resulting in a more Poissonian distribution. Conversely, smaller regions have highly nonrandom time series and show two distinct bumps in their interevent time distributions. For intermediate values of μ, the crossover between the correlated and uncorrelated curves can result in an apparent power law in the overall distribution, whose exponent does not have a simple relationship to any of the ETAS parameters. Artificially selecting stationary periods from a time series that is fundamentally nonstationary on the time scale considered introduces a strong sample bias that takes the form of an apparently universal gamma distribution. The true dependence of the distribution just on region size—ignoring different effective branching ratios from one region to another—is too complicated to fulfil a simple unified scaling law.

We would like to acknowledge the UK Engineering and Physical Sciences Research Council for funding S. T. on a Doctoral Training grant and M. N. on GR/T11753/01.

*s.touati-2@sms.ed.ac.uk

[1] P. Bak, K. Christensen, L. Danon, and T. Scanlon, Phys. Rev. Lett. **88**, 178501 (2002).
[2] A. Corral, Phys. Rev. E **68**, 035102(R) (2003).
[3] A. Corral, Phys. Rev. Lett. **92**, 108501 (2004).
[4] J. Davidsen and C. Goltz, Geophys. Res. Lett. **31**, L21612 (2004).
[5] R. Shcherbakov, G. Yakovlev, D. L. Turcotte, and J. B. Rundle, Phys. Rev. Lett. **95**, 218501 (2005).
[6] G. Molchan, Pure Appl. Geophys. **162**, 1135 (2005).
[7] L. de Arcangelis, E. Lippiello, C. Godano, and M. Nicodemi, Eur. Phys. J. B **64**, 551 (2008).
[8] S. Lennartz, V. N. Livina, A. Bunde, and S. Havlin, Europhys. Lett. **81**, 69001 (2008).
[9] J. Davidsen, S. Stanchits, and G. Dresen, Phys. Rev. Lett. **98**, 125502 (2007).
[10] V. Carbone, L. Sorriso-Valvo, P. Harabaglia, and I. Guerra, Europhys. Lett. **71**, 1036 (2005).
[11] Y. Ogata, J. Am. Stat. Assoc. **83**, 9 (1988).
[12] A. Saichev and D. Sornette, Phys. Rev. Lett. **97**, 078501 (2006).
[13] A. Saichev and D. Sornette, J. Geophys. Res. **112**, B04313 (2007).
[14] G. Molchan and T. Kronrod, Pure Appl. Geophys. **164**, 75 (2007).
[15] M. Lindman, K. Jonsdottir, R. Roberts, B. Lund, and R. Bodvarsson, Phys. Rev. Lett. **94**, 108501 (2005).
[16] D. Sornette, S. Utkin, and A. Saichev, Phys. Rev. E **77**, 066109 (2008).
[17] M. Naylor, I. Main, and S. Touati, J. Geophys. Res. **114**, B01316 (2009).
[18] I. G. Main, J. McCloskey, M. Naylor, and L. Li, Nature Geoscience **1**, 142 (2008).
[19] A. Helmstetter and D. Sornette, J. Geophys. Res. **107**, 2237 (2002).
[20] M. Huc and I. G. Main, J. Geophys. Res. **108**, 2324 (2003).
[21] S. Hainzl, F. Scherbaum, and C. Beauval, Bull. Seismol. Soc. Am. **96**, 313 (2006).
[22] K. Jonsdottir, M. Lindman, R. Roberts, B. Lund, and R. Bodvarsson, Tectonophysics **424**, 195 (2006).